HHS Public Access

Author manuscript

Brain Stimul. Author manuscript; available in PMC 2019 April 29.

Published in final edited form as:

Brain Stimul. 2018 ; 11(3): 492–500. doi:10.1016/j.brs.2017.12.009.

Neurophysiologic effects of transcutaneous auricular vagus nerve stimulation (taVNS) via electrical stimulation of the tragus: A concurrent taVNS/fMRI study and review

Bashar W. Badran[a,b,c,d,*], **Logan T. Dowdle**[a,b], **Oliver J. Mithoefer**[b], **Nicholas T. LaBate**[e], **James Coatsworth**[f], **Joshua C. Brown**[b,g], **William H. DeVries**[b], **Christopher W. Austelle**[b], **Lisa M. McTeague**[b], and **Mark S. George**[a,b,f,g,h]

[a]Department of Neuroscience, Medical University of South Carolina, Charleston, SC, 29425, United States

[b]Department of Psychiatry, Medical University of South Carolina, Charleston, SC, 29425, United States

[c]Department of Psychology, University of New Mexico, Albuquerque, NM, 87131, United States

[d]US Army Research Lab, Aberdeen Proving Ground, MD, 21005, United States

[e]College of Charleston, Charleston, SC, 29403, United States

[f]Center for Biomedical Imaging, Medical University of South Carolina, Charleston, SC, 29425, United States

[g]Department of Neurology, Medical University of South Carolina, Charleston, SC, 29425, United States

[h]Ralph H. Johnson VA Medical Center, Charleston, SC, 29401, United States

Abstract

Background: Electrical stimulation of the auricular branch of the vagus nerve (ABVN) via transcutaneous auricular vagus nerve stimulation (taVNS) may influence afferent vagal networks. There have been 5 prior taVNS/fMRI studies, with inconsistent findings due to variability in stimulation targets and parameters.

Objective: We developed a taVNS/fMRI system to enable concurrent electrical stimulation and fMRI acquisition to compare the effects of taVNS in relation to control stimulation.

Methods: We enrolled 17 healthy adults in this single-blind, crossover taVNS/fMRI trial. Based on parameters shown to affect heart rate in healthy volunteers, participants received either left tragus (active) or earlobe (control) stimulation at 500 μs 25 HZ for 60 s (repeated 3 times over 6 min). Whole brain fMRI analysis was performed exploring the effect of: active stimulation, control stimulation, and the comparison. Region of interest analysis of the midbrain and brainstem was also conducted.

[*]Corresponding author. MUSC Institute of Psychiatry, 67 President St., 504N, Charleston, SC, 29425, United States. badran@musc.edu (B.W. Badran).

Results: Active stimulation produced significant increased BOLD signal in the contralateral postcentral gyrus, bilateral insula, frontal cortex, right operculum, and left cerebellum. Control stimulation produced BOLD signal activation in the contralateral postcentral gyrus. In the active vs. control contrast, tragus stimulation produced significantly greater BOLD increases in the right caudate, bilateral anterior cingulate, cerebellum, left prefrontal cortex, and mid-cingulate.

Conclusion: Stimulation of the tragus activates the cerebral afferents of the vagal pathway and combined with our review of the literature suggest that taVNS is a promising form of VNS. Future taVNS/fMRI studies should systematically explore various parameters and alternative stimulation targets aimed to optimize this novel form of neuromodulation.

Keywords

Transcutaneous auricular vagus nerve stimulation (taVNS); fMRI; Ear stimulation; Anterior cingulate cortex (ACC)

Introduction

Cervical vagus nerve stimulation (VNS) involves direct implantation of stimulating electrodes, wires, and a pulse generator, which electrically stimulates the left cervical bundle of the vagus nerve, Cranial Nerve X (CN X). Cervical VNS is a relatively safe and moderately effective therapy for treating intractable epilepsy or treatment resistant depression [1,2]. Unfortunately, risks involved in surgical implantation, as well as high procedural cost ($30,000–50,000) makes it less appealing, and limits access. This is especially so if insurance companies do not reimburse the procedure (as is currently the case regarding VNS to treat depression). Additionally, only about 30% of implanted patients demonstrate a clinical response, despite undergoing the procedure. A non-invasive method to stimulate the vagus as an alternative treatment, or to determine ultimate VNS responders before they have cervical surgery would likely improve VNS use as a treatment modality.

The numerous behavioral benefits of cervical VNS likely arise from its highly diffuse afferent brain targets. The vagus nerve enters the central nervous system in the nucleus tractus solitarius (NTS) [3,4] (Fig. 1). From the NTS, there are direct afferent projections to the parabrachial complex (PB); from here, projections are sent to the locus coeruleus (LC) and raphe nuclei [5]. Further ascending projections from the PB ascend to higher brain regions [6]. Interestingly, Krahl et al. lesioned the LC and caused the anti-epileptic effect of VNS to disappear [7], demonstrating the role of the norepinephrine (NE) released by the LC as central to the mechanism of anti-epileptic VNS. NE is not the only neurotransmitter involved in the afferent vagal pathway. Serotonin (5-HT) is released through direct projections from the dorsal raphe nucleus [8], the primary source of serotonin, which independently has a wide range of ascending brain targets (thalamus, cerebellum, hypothalamus, amygdala, insula, cingulate and frontal cortex), many of which are also targeted by the ascending LC pathway (Fig. 1).

Aside from NE and 5-HT, which are often described as the key neurotransmitters involved in VNS, a dopaminergic basis of response has been suggested. A recent study by Conway and colleagues used ^{17}Fluorodeoxyglucose positron emission tomography (PET) imaging in

humans to reveal VNS responder-specific increased activation of the ventral tegmental area (VTA), one of two regions responsible for dopamine (DA) release [9]. Non-responders were not shown to have this increase, suggesting DA may be an alternative VNS mechanism. Only DA metabolites (not NE or 5-HT) were also reported to be increased in cerebrospinal fluid (CSF) after VNS therapy [10].

The auricular branch of the vagus nerve (ABVN) spans from the main bundle of the vagus nerve and innervates the human ear, although its afferent projections are still not well understood. The ABVN is the target of a novel form of noninvasive brain stimulation, known as transcutaneous auricular vagus nerve stimulation (taVNS). Modern taVNS was perhaps first described by Ventureyra in 2000 [11], with several more recent studies using this novel form of neuromodulation [12–17], including 5 preliminary fMRI trials [18–22]. Importantly, these taVNS/fMRI trials have widely different methodology with varied results. For example, the studies employed a range of stimulation targets, parameters, durations, and control site. The field of taVNS still lacks a consensus on which parameters and ear targets are the most biologically active, and whether the brain regions secondarily activated depend on specific parameters. That is, can one sculpt the central brain activation of taVNS by simply varying target and dose parameters? To better visualize this, we have overlaid the various prior studies' parameters and brain activations on Fig. 1.

Currently, there is a debate as to which anatomical target is most biologically active. There has been only one human auricle dissection study to date conducted in 7 German cadavers [23] that demonstrates the cymba conchae and tragus as the highest density of ABVN projections. Groups have conducted studies stimulating both tragus and cymba conchae in fMRI paradigms, with both sites delivering promising results. Without intricate microdissection and combined stimulation studies, along with individual anatomical differences, it is difficult to determine which site truly activates the main bundle of the vagus. It is also important to consider stimulation parameters in VNS paradigms, as Mu et al. demonstrated that increasing pulse width of cervically implanted VNS increases BOLD signal activation in the vagal network [24]. Similar to cervical VNS, taVNS likely varies as a function of stimulation characteristics and thus should be assessed parametrically.

Our group has conducted a series of safety and parametric physiological work demonstrating the autonomic effects of electrical stimulation of the tragus. These findings suggest the tragus is a likely, biologically active target [25]. We proceeded to develop a taVNS system that is compatible with functional magnetic resonance imaging (fMRI) in order to further test the afferent brain activation of electrical stimulation of the tragus. Using this novel technique and the parameters that produced heart rate changes, we conducted a concurrent taVNS/fMRI imaging study to determine the afferent pathway of left tragus stimulation in healthy adults.

Methods

Overview

We conducted a two-visit, single blind, crossover fMRI trial exploring the effects of active taVNS stimulation compared to control earlobe stimulation. Participants had two identical

scanning visits, separated by at least one day to avoid carryover effects. Scans were acquired at the MUSC Center for Biomedical Imaging research dedicated 3T Siemens Trio location. This study was approved by the MUSC Institutional Review Board (IRB) and is registered on ClinicalTrials.org (NCT02835885). All participants signed written informed consent prior to scanning.

Participants and inclusion criteria

17 healthy individuals (8 women) were enrolled after meeting the following inclusion criteria: Age 18–45, no personal or family history of seizure, mood, or cardiovascular disorders, no facial or ear pain, no recent ear trauma, no metal implants including pacemakers, not pregnant, no dependence on alcohol or recent illicit drug use, not taking any pharmacological agents known to increase seizure risk (e.g., bupropion, neuroleptics, albuterol, theophylline, antidepressants, thyroid medications, or stimulants) and MRI contraindications (e.g., metal in body, pregnancy, and claustrophobia).

fMRI scanning

All MRI scanning was conducted using a Siemens Trio TIM 3.0T system and a 32-Channel head coil. Individuals were positioned head-first supine in the MRI scanner, and foam pads were used to stabilize their heads and to minimize movement.

Each of the two scanning sessions lasted approximately 30 min, during which multiple scanning sequences were acquired (Fig. 2a). First, for the purpose of warping each participant into a standard space template, a high resolution anatomical MPRAGE (TR:1900 ms; TE: 2.26 ms; Voxel size: 1 mm^3; 208 slices, FA: 9 deg) was collected. Following the anatomical image, three identical taVNS/fMRI scans were collected, during which participants received either active or control concurrent taVNS. Lastly, a field map was acquired to correct for distortions due to magnetic field inhomogeneity.

The concurrent taVNS/fMRI scans were conducted using echo-planar imaging (EPI) sequence (TR: 2800 ms; TE: 35 ms; Voxel size: 3.0 mm^3; 47 slices, FA: 76 deg) in a block design described in Fig. 2b. Each scan run was identical, consisting of three 60s “ON” periods, each separated by 60s “OFF” periods. A 30s “OFF” period also preceded the first and proceeded the last “ON” periods. Scans totaled 6 min each. The stimulation was synchronized with the start of each taVNS/fMRI BOLD sequence acquisition (from 0:00 and ran to 6:00 for each taVNS/fMRI run), and was triggered upon first fMRI volume acquisition using an automated stimulation system delivering TTL pulses to the constant current stimulator at a specific frequency and duration. Timing validation was confirmed with the console timer after each individual stimulation session. Upon completion of each taVNS/fMRI scan, individuals were asked via intercom how many stimulation blocks they sensed in order to verify signal transmission into the scanner and all three “ON” blocks were delivered. Participants were also asked to rate their pain on a visual response scale (NRS) from one (no pain) to ten (extreme pain).

Concurrent taVNS/fMRI system

Stimulation was delivered via custom developed stimulating electrodes pictured in Fig. 3a +b. The design of the electrodes was based on a freely available clip design (Clip by J_Hodgie, creative commons non-commercial attribution, www.thingiverse.com/thing:5580) and modified in order to fit round metal electrodes at the clip ends. Computer assisted drawings of the electrode clamps were generated in SketchUp (Timble Navigation, USA) and subsequently 3D-printed in ABS plastic at the MUSC Brain Stimu-lation Laboratory. The round, unipolar stimulation electrodes were 1 cm in diameter, made of Ag/AgCl, and affixed to the 3D-printed clamps using cyanoacrylate. Copper was used for all wiring. Ten20 conductive paste was used as a conductor for the electrodes.

Constant current stimulation was delivered using a Digitimer DS7a set to <400 V. Lead wires were attached to the Digitimer output and connected to a radio frequency (RF) patch panel in the wall between the equipment room and magnet room using a serial connector on both sides. Fig. 3c shows the taVNS/fMRI setup. Wire was run from the patch panel in the magnet room towards the foot of the MRI scanner, where it was then run on top of the participant who was laying supine head first on the scanning table. 1/2-inch PVC piping was used to insulate the wires, and rested on the participant's abdomen. Stimulation electrodes were clamped to the individual's tragus or earlobe, depending on active or control condition.

taVNS parameters and stimulation targets

The parameters used for this fMRI trial were 500 μs 25 Hz (monophasic square waves) based on previous autonomic effects (manuscript under review and attached for reviewers). Perceptual threshold (PT) was determined while the participant was laying in the scanner with electrodes attached. Stimulation current was later set to 200% of PT. Perception of stimulation was relayed to the equipment room via intercom, and the current was calibrated to the minimum perceptual level for each participant. Active stimulation was delivered to the left tragus, control stimulation to the left earlobe (Fig. 2c).

Data processing and analysis

All images were converted from DICOM to NifTI using dcm2nii applet. All further processing and analysis were performed in SPM 12 software (UCL) using MATLAB R2012a (The MathWorks Inc, Natick, MA). First, normalization parameters were derived from the segmentation of the whole brain anatomical images. Skull stripped anatomical images were created to improve functional to anatomical coregistration. Next, the functional images were realigned to reduce motion related variance. The mean image from realignment was coregistered to the skull stripped anatomical image using a normalized mutual information algorithm. The estimated coregistration parameters were combined with the normalization parameters in a single step and applied to the functional data. Finally, the data was smoothed using an 8 mm FWHM Gaussian smoothing kernel. No participants were excluded on the basis of the estimated movement parameters.

Three stimulation “ON” periods were modeled (onset times: 30s, 150s, 270s; duration 60s) in a block design. At the subject level, “ON” blocks were convolved with the canonical hemodynamic response function provided by SPM12. Contrast maps of “ON” stimulation

were carried forward into a second level model, for group-level analysis of condition effects. Single sample t-tests of all individual stimulation blocks were considered in relation to the implicit baseline (active: ON > OFF, ON < OFF; control: ON > OFF, ON < OFF). An overall taVNS paired t-test contrast was also conducted (active ON > OFF > control ON > OFF; active ON<OFF > control ON < OFF). Lastly, a mask was created to explore the brain stem regional activations on all of the second level analyses.

Results

Participants, stimulation, and tolerability

All 17 healthy, right-handed individuals (8 women, mean age ± SD years: 25.8 ± 7.59) completed both visits without any dropouts and were included in the analysis. Mean perceptual thresholds (PT) are as follows (mean ± SD mA): tragus 1.57 ± 0.48; earlobe 1.22 ± 0.58. The current at which taVNS was delivered was a scale multiplier of the PT (200%). Mean stimulation currents were as follows (mean ± SD mA): tragus 3.14 ± 0.99; earlobe 2.43 ± 1.16. Using a 2-tailed paired *t*-test, there was no significant difference in perceptual threshold between the two stimulation sites ($p > .05$) (Table 1). Mean numeric rating scale (NRS) pain scores for both active and control conditions were low, with active stimulation rating a mean NRS difference of 0.6 higher on a subjective 1–10 scale in 0.5 increments than control (Table 1). Although a paired *t*-test revealed that this difference in pain ratings is significant ($p < .01$), in practicality this stimulation would be considered and painless and not clinically meaningful in both conditions, as the mean difference was less than one rating point and the maximum pain rated by any individual was two points [26].

Group-level whole-brain fMRI analysis

Earlobe (control condition) stimulation only—During left earlobe stimulation, statistically significant increases in BOLD signal (ON > OFF) were found in the right inferior postcentral gyrus, operculum, and insula (one sample *t*-test, $p < .005$ FWE corrected, extent threshold = 100 voxels) (Fig. 4a, Table 2). There were no findings in the opposite direction (ON < OFF contrast).

Tragus (active condition) stimulation only—During left tragus stimulation condition, statistically significant increases in BOLD signal (ON > OFF) were found in similar areas as earlobe stimulation (right postcentral gyrus, operculum, and insula) as well as other more diffuse activations such as the left insula, angular gyrus, cerebellum, and bilateral frontal lobes ($n = 17$, one sample *t*-test, $p < .05$ FWE corrected, cluster forming threshold $P < .005$, extent threshold = 100 voxels) (Fig. 4b, Table 2). No significant deactivations were found (ON < OFF contrast).

Tragus (active) greater than earlobe (control) (between conditions)—The effect of control stimulation was directly contrasted to active stimulation. Significant BOLD increases during tragus stimulation as opposed to earlobe stimulation were revealed in the right mid-cingulate, caudate, bilateral operculum, bilateral cerebellum, and bilateral anterior cingulate cortex (ACC) (paired *t*-test, $p < .05$ FWE corrected, cluster forming threshold $P < .$

005, extent threshold = 100 voxels) (Fig. 5, Table 2). No BOLD signal deactivations were revealed (ON < OFF contrast).

Brain stem analysis—A region of interest brainstem analysis was conducted using an explicit mask comprising the pons, midbrain, and medulla [27]. No significant findings were revealed in any of the groups analyzed (active only, control only, active > control).

Discussion

We investigated the direct brain effects of taVNS to either the left tragus (active) or earlobe (control) using a novel taVNS/fMRI paradigm in 17 healthy individuals. Each participant attended two scanning sessions, in which both left tragus (active) and left earlobe (control) stimulation was administered in order to determine the afferent brain effects of electrical stimulation of the ABVN. Our findings reveal that active taVNS in healthy young adults at 500 μs 25 Hz delivered for 60 s repeated 3 times over 6 min produces significant BOLD activations throughout cortical, subcortical, and cerebellar brain regions associated with the afferent vagal pathway. In contrast, control stimulation of the earlobe exclusively produces a contralateral somatosensory BOLD signal response in the postcentral gyrus representation of the face. When control response is subtracted from the active response in the overall contrast of active > control, significant activations emerge throughout the cingulate gyrus (bilateral ACC, bilateral mid-cingulate), frontal cortex (left middle and frontal gyrus), cerebellum, and right caudate. These activations are presumably due to stimulation of vagus afferents arising from the ear.

Within this trial, we describe two effects: 1) the somatosensory cortical representation of the ear, and 2) the cortical and subcortical direct brain effects of stimulating the ABVN. Penfield described the homuncular representation of the human primary sensory cortex [28], and notably the ear is omitted from these trials. To date only been two studies have explored ear somatosensory representation [29,30], the first using magnetoencephalography (MEG) and the second using fMRI. Similar to the results in the current study, both describe the somatosensory response of the left ear being represented on the contralateral somatosensory cortex in the face and neck areas. The MEG findings demonstrated that somatosensory evoked magnetic fields (SEFs) were produced in response to slow (1 Hz), ultra brief (0.05 ms pulse width) electrical stimulation of the earlobe. The follow-up MRI findings by the same group confirm initial MEG findings that slow (2 Hz), brief (0.5 ms pulse width) electrical stimulation solely activates contralateral postcentral gyrus. Although our stimulation current was faster (25 Hz compared to 1 and 2 Hz), the pulse width was identical and our control stimulation findings are similar to these two sequential trials conducted by Nihashi et al.

The afferent pathway of the ABVN is still poorly understood, although we hypothesize that it activates the main vagal afferent pathway (via the NTS, LC, and upstream cortical projections) [7,31–33]. To date, including this trial, there have been six taVNS/ fMRI studies exploring the direct brain effects of electrical stimulation to the ear (Table 3). Findings vary widely, as do the methods. As demonstrated in prior cervical VNS/fMRI trials, parameters have a direct effect on BOLD response [34]. However, two of the prior taVNS trials

explored 250 μs pulse width stimulation [20,21] and two others administered 20 μs stimulation [18,19]. Our trial used a 500 μs 25 Hz parameter similar to Yakunina et al. [22], with similar findings. Like the Yakunina group, we demonstrate that tragus stimulation produces significant increased activation in the angular gyrus, caudate, cerebellum, cingulate, and frontal cortex. These regions in general are also found to be activated throughout the other shorter pulse width trials listed in Table 3 and are afferent targets of the vagus nerve pathway, suggesting that ABVN stimulation enters the vagal bundle and projects to the brain via the brainstem.

Another major difference between these trials was the duration of stimulation, or “ON” period, during scanning. Three studies stimulated for less than one minute [18,19,21], while the most recent trials stimulated for six and seven minutes, respectively [20,22]. In our trial, stimulation was delivered for one-minute blocks. The studies utilizing long stimulation periods reported BOLD signal activations in the brainstem region, while the prior three trials did not. Even in ideal conditions, breathing, heart rate, subject motion, and swallowing artifacts make imaging the small brainstem regions such as the LC and NTS a challenge. It is plausible that we did not discover any brainstem activations due to our short stimulation period of one minute, or due to our whole brain imaging approach (larger slices for wider brain coverage). Future studies should consider longer stimulation periods and scans optimized for imaging with rapid, thin slice acquisition of those regions, rather than whole brain scans if imaging of brainstem nuclei is a goal.

Interestingly, of all prior studies, ours is the only one that reflects the bilateral activation of the ACC and left dorsolateral pre-frontal cortex (DLPFC) via taVNS. This may reveal a potential mechanism for the anti-depressant effect of cervically implanted VNS as well as the proposed anti-depressant effect of taVNS that has been described in the literature [17,35,36]. The ACC is involved in cognition and emotional processing [37,38] and may play a key role in the depressions, expressing reduced glutamate release [39–41] and reduced glial cell density [42–44] in pathologic conditions. The ACC also has been used as a longitudinal predictor of treatment response in depression [45,46]. The left DLPFC has been demonstrated to be hypoactive in depression [47,48] and is a target of high frequency rTMS for its treatment [49–52]. Strong bilateral insular activity in the active contracts compared to control stimulation may also be of importance, as the insula has been implicated as a key region in models of biomarkers for mood disorders [53,54]. Presented with significant BOLD activations in regions of the brain associated with major depressive disorder (MDD), it is reasonable to consider taVNS as approach to treating MDD.

This trial establishes the left tragus as a biologically active ear stimulation site, allowing for transcutaneous stimulation of the ABVN and its afferent vagal network. The parameters used in this study (500 μs, 25 Hz, 60s ON, 60s OFF) are revealed to significantly activate these networks and produce reliable activation of vagal afferent networks. These findings are similar to the Yakunina group findings [22], which is the only prior study that employed the 500 μs 25 Hz parameter. Our suggested duty cycle (1min on/ 1min off) is tolerable and can be easily translated into a disease population.

Limitations

It is important to address three limitations of our study we believe are critical in guiding future taVNS development. Unlike other studies by Frangos and Yakunina, our findings did not reveal any brainstem activation in the regions known to be the vagus entrance into the CNS such as the NTS or LC due to methodological constraints. The human LC is a remarkably small brain region, measuring roughly 1–2 mm at widest in the axial plane [55]. It is difficult to image such small regions without conducting advanced imaging techniques utilizing rapid, thin slice acquisitions targeting strictly the brainstem. Our scanning sequences were optimized to capture the whole brain hemodynamics at a voxel size of 3 mm^3 which limits the ability to capture not only the structural detail of the NTS and LC, but also its fMRI BOLD response. Future studies should employ specific advanced taVNS/fMRI midbrain and brainstem imaging as well as whole brain scanning.

Our active stimulation site was the left tragus and control region the earlobe. This was based on a series of autonomic studies conducted by our group investigating the effects of tragus stimulation. We cannot determine whether the tragus is the optimal taVNS target as we did not include a cymba conchae target. Both the cymba conche and tragus have been suggested to be biologically active sites and future studies should explore these targets in a head to head fashion to determine optimal stimulation site.

Lastly, our taVNS duty cycle was chosen to be consistent with our prior physiological trials outside of the scanner. The safety profile of stimulation longer than one minute was unknown and we did not want to risk adverse events in the MRI scanner, although upon completing this trial, we believe that stimulation periods longer than 60s would introduce minimal safety risk and would potentially illicit a measurable brainstem BOLD response as demonstrated by Frangos and Yakinuna. There may also be residual cortical brain effects persisting in the 60s inter-stimulation rest blocks that we cannot control for due to scanning procedural constraints. However this type of design was used to increase the power of our effect by increasing the number of stimulation blocks while minimizing scanner drift inherent in long stimulation trials.

Conclusion

These findings demonstrate that taVNS (delivered at 500 μs, 25 Hz) to the left tragus for one minute produces significant cortical effects in the vagal afferent pathway compared to control stimulation of the earlobe. These findings are similar to prior taVNS imaging studies revealing that stimulating the ear at specific regions thought to have ABVN innervations activate afferent vagal networks. Future taVNS/fMRI trials are needed to explore the effects of changes in stimulation parameters on the BOLD signal response.

Acknowledgements

The authors would like to thank Minnie Dobbins for her help in organizing and coordinating these trials and the MUSC Brain Stimulation Laboratory for their funding and the MUSC Center for Biomedical Imaging for contributing MRI scanner time. Truman Brown and Jaycee Doose assisted in the pre-trial development.

Financial support from: NIH R21/R33 (5R21MH106775-02), National Center of Neuromodulation for Rehabilitation (NC NM4R) (5P2CHD086844-03), COBRE Brain Stimulation Core (5P20GM109040-04).

References

[1]. Ben-Menachem E, Mañon-Espaillat R, Ristanovic R, Wilder B, Stefan H, Mirza W, et al. Vagus nerve stimulation for treatment of partial seizures: 1. A controlled study of effect on seizures. Epilepsia 1994;35(3):616–26. [PubMed: 8026408]

[2]. Handforth A, DeGiorgio C, Schachter S, Uthman B, Naritoku D, Tecoma E, et al. Vagus nerve stimulation therapy for partial-onset seizures a randomized active-control trial. Neurology 1998;51(1):48–55. [PubMed: 9674777]

[3]. Benarroch EE, editor. The central autonomic network: functional organization, dysfunction, and perspective Mayo Clin Proc. Elsevier; 1993.

[4]. Kalia M, Sullivan JM. Brainstem projections of sensory and motor components of the vagus nerve in the rat. JComp Neurol 1982;211(3):248–64. [PubMed: 7174893]

[5]. Van Bockstaele EJ, Peoples J, Valentino RJ. Anatomic basis for differential regulation of the rostrolateral peri–locus coeruleus region by limbic afferents. Biol Psychiatr 1999;46(10):1352–63.

[6]. Henry TR. Therapeutic mechanisms of vagus nerve stimulation. Neurology 2002;59(6 suppl 4):S3–14.

[7]. Krahl SE, Clark KB, Smith DC, Browning RA. Locus coeruleus lesions suppress the seizure-attenuating effects of vagus nerve stimulation. Epilepsia 1998;39(7):709–14. [PubMed: 9670898]

[8]. Dong J, Debonnel G. Enhancement of the function of rat serotonin and norepinephrine neurons by sustained vagus nerve stimulation. J Psychiatr Neurosci 2009;34(4):272.

[9]. Conway CR, Chibnall JT, Cumming P, Mintun MA, Gebara MAI, Perantie DC, et al. Antidepressant response to aripiprazole augmentation associated with enhanced FDOPA utilization in striatum: a preliminary PET study. Psychiatr Res 2014;221(3):231–9.

[10]. Carpenter LL, Tyrka AR, McDougle CJ, Malison RT, Owens MJ, Nemeroff CB, et al. Cerebrospinal fluid corticotropin-releasing factor and perceived early-life stress in depressed patients and healthy control subjects. Neuropsychopharmacology 2004;29(4):777. [PubMed: 14702025]

[11]. Ventureyra EC. Transcutaneous vagus nerve stimulation for partial onset seizure therapy. Child's Nerv Syst 2000;16(2):101–2. [PubMed: 10663816]

[12]. Capone F, Assenza G, Di Pino G, Musumeci G, Ranieri F, Florio L, et al. The effect of transcutaneous vagus nerve stimulation on cortical excitability. J Neural Transm (Vienna) 2015;122(5):679–85. [PubMed: 25182412]

[13]. Kreuzer PM, Landgrebe M, Husser O, Resch M, Schecklmann M, Geisreiter F, et al. Transcutaneous vagus nerve stimulation: retrospective assessment of cardiac safety in a pilot study. Front Psychiatr 2012;3:70.

[14]. Kreuzer PM, Landgrebe M, Resch M, Husser O, Schecklmann M, Geisreiter F, et al. Feasibility, safety and efficacy of transcutaneous vagus nerve stimulation in chronic tinnitus: an open pilot study. Brain Stimul 2014;7(5):740–7. [PubMed: 24996510]

[15]. Clancy JA, Mary DA, Witte KK, Greenwood JP, Deuchars SA, Deuchars J. Non-invasive vagus nerve stimulation in healthy humans reduces sympathetic nerve activity. Brain Stimul 2014;7(6):871–7. [PubMed: 25164906]

[16]. Lehtimaki J, Hyvarinen P, Ylikoski M, Bergholm M, Makela JP, Aarnisalo A, et al. Transcutaneous vagus nerve stimulation in tinnitus: a pilot study. Acta Otolaryngol 2013;133(4):378–82. [PubMed: 23237096]

[17]. Hein E, Nowak M, Kiess O, Biermann T, Bayerlein K, Kornhuber J, et al. Auricular transcutaneous electrical nerve stimulation in depressed patients: a randomized controlled pilot study. J Neural Transm 2013;120(5):821–7. [PubMed: 23117749]

[18]. Kraus T, Hösl K, Kiess O, Schanze A, Kornhuber J, Forster C. BOLD fMRI deactivation of limbic and temporal brain structures and mood enhancing effect by transcutaneous vagus nerve stimulation. J Neural Transm 2007;114(11):1485–93. [PubMed: 17564758]

[19]. Kraus T, Kiess O, Hösl K, Terekhin P, Kornhuber J, Forster C. CNS BOLD fMRI effects of sham-controlled transcutaneous electrical nerve stimulation in the left outer auditory canal–a pilot study. Brain Stimul 2013;6(5):798–804. [PubMed: 23453934]

[20]. Frangos E, Ellrich J, Komisaruk BR. Non-invasive access to the vagus nerve central projections via electrical stimulation of the external ear: fMRI evidence in humans. Brain Stimul 2015;8(3): 624–36. [PubMed: 25573069]

[21]. Dietrich S, Smith J, Scherzinger C, Hofmann-Preiß K, Freitag T, Eisenkolb A, et al. A novel transcutaneous vagus nerve stimulation leads to brainstem and cerebral activations measured by functional MRI/Funktionelle Magnet-resonanztomographie zeigt Aktivierungen des Hirnstamms und weiterer zerebraler Strukturen unter transkutaner Vagusnervstimulation. Biomed Tech/ Biomed Eng 2008;53(3):104–11.

[22]. Yakunina N, Kim SS, Nam EC. Optimization of transcutaneous vagus nerve stimulation using functional MRI. Neuromodulation Technol Neural Interface 2017 4 1;20(3):290–300.

[23]. Peuker ET, Filler TJ. The nerve supply of the human auricle. Clin Anat 2002;15(1):35–7. [PubMed: 11835542]

[24]. Mu Q, Bohning DE, Nahas Z, Walker J, Anderson B, Johnson KA, et al. Acute vagus nerve stimulation using different pulse widths produces varying brain effects. Biol Psychiatr 2004;55(8):816–25.

[25]. Badran B, Glusman C, Badran A, Austelle C, DeVries W, Borckhardt J, et al. The physiological and neurobiological effects of transcutaneous auricular vagus nerve stimulation (taVNS). Brain Stimul 2017;10(2):378.

[26]. Hawker GA, Mian S, Kendzerska T, French M. Measures of adult pain: visual analog scale for pain (VAS Pain), numeric rating scale for pain (NRS Pain), McGill pain questionnaire (MPQ), short-form McGill pain questionnaire (SF-MPQ), chronic pain grade scale (CPGS), short Form-36 bodily pain scale (SF-36 BPS), and measure of intermittent and constant osteoarthritis pain (ICOAP). Arthritis Care Res 2011;63(Suppl 11):S240–52.

[27]. Maldjian JA, Laurienti PJ, Kraft RA, Burdette JH. An automated method for neuroanatomic and cytoarchitectonic atlas-based interrogation of fMRI data sets. Neuroimage 2003;19(3):1233–9. [PubMed: 12880848]

[28]. Penfield W, Boldrey E. Somatic motor and sensory representation in the cerebral cortex of man as studied by electrical stimulation. Brain J Neurol 1937.

[29]. Nihashi T, Kakigi R, Kawakami O, Hoshiyama M, Itomi K, Nakanishi H, et al. Representation of the ear in human primary somatosensory cortex. Neuroimage 2001;13(2):295–304. [PubMed: 11162270]

[30]. Nihashi T, Kakigi R, Okada T, Sadato N, Kashikura K, Kajita Y, et al. Functional magnetic resonance imaging evidence for a representation of the ear in human primary somatosensory cortex: comparison with magnetoencephalography study. Neuroimage 2002;17(3):1217–26. [PubMed: 12414262]

[31]. Lulic D, Ahmadian A, Baaj AA, Benbadis SR, Vale FL. Vagus nerve stimulation. Neurosurg Focus 2009;27(3):E5.

[32]. Valdés-Cruz A, Magdaleno-Madrigal VM, Martinez-Vargas D, Fernández-Mas R, Almazán-Alvarado S, Martinez A, et al. Chronic stimulation of the cat vagus nerve: effect on sleep and behavior. Prog Neuropsychopharmacol Biol Psychiatr 2002;26(1):113–8.

[33]. Groves DA, Brown VJ. Vagal nerve stimulation: a review of its applications and potential mechanisms that mediate its clinical effects. Neurosci Biobehav Rev 2005;29(3):493–500. [PubMed: 15820552]

[34]. Lomarev M, Denslow S, Nahas Z, Chae J-H, George MS, Bohning DE. Vagus nerve stimulation (VNS) synchronized BOLD fMRI suggests that VNS in depressed adults has frequency/dose dependent effects. J Psychiatr Res 2002;36(4):219–27. [PubMed: 12191626]

[35]. Sackeim HA, Rush AJ, George MS, Marangell LB, Husain MM, Nahas Z, et al. Vagus nerve stimulation (VNS™) for treatment-resistant depression: efficacy, side effects, and predictors of outcome. Neuropsychopharmacology 2001;25(5):713–28. [PubMed: 11682255]

[36]. Rush AJ, George MS, Sackeim HA, Marangell LB, Husain MM, Giller C, et al. Vagus nerve stimulation (VNS) for treatment-resistant depressions: a multi-center study. Biol Psychiatr 2000;47(4):276–86.

[37]. Bush G, Luu P, Posner MI. Cognitive and emotional influences in anterior cingulate cortex. Trends Cognit Sci 2000;4(6):215–22. [PubMed: 10827444]

[38]. MacDonald AW, Cohen JD, Stenger VA, Carter CS. Dissociating the role of the dorsolateral prefrontal and anterior cingulate cortex in cognitive control. Science 2000;288(5472):1835–8. [PubMed: 10846167]

[39]. Auer DP, Pütz B, Kraft E, Lipinski B, Schill J, Holsboer F. Reduced glutamate in the anterior cingulate cortex in depression: an in vivo proton magnetic resonance spectroscopy study. Biol Psychiatr 2000;47(4):305–13.

[40]. Rosenberg DR, Mirza Y, Russell A, Tang J, Smith JM, Banerjee SP, et al. Reduced anterior cingulate glutamatergic concentrations in childhood OCD and major depression versus healthy controls. J Am Acad Child Adolesc Psychiatr 2004;43(9):1146–53.

[41]. Rosenberg DR, MacMaster FP, Mirza Y, Smith JM, Easter PC, Banerjee SP, et al. Reduced anterior cingulate glutamate in pediatric major depression: a magnetic resonance spectroscopy study. Biol Psychiatr 2005;58(9):700–4.

[42]. Cotter D, Mackay D, Landau S, Kerwin R, Everall I. Reduced glial cell density and neuronal size in the anterior cingulate cortex in major depressive disorder. Arch Gen Psychiatr 2001;58(6): 545–53. [PubMed: 11386983]

[43]. Cotter DR, Pariante CM, Everall IP. Glial cell abnormalities in major psychiatric disorders: the evidence and implications. Brain Res Bull 2001;55(5):585–95. [PubMed: 11576755]

[44]. Öngür D, Drevets WC, Price JL. Glial reduction in the subgenual prefrontal cortex in mood disorders. Proc Natl Acad Sci USA 1998;95(22):13290–5. [PubMed: 9789081]

[45]. Pizzagalli D, Pascual-Marqui RD, Nitschke JB, Oakes TR, Larson CL, Abercrombie HC, et al. Anterior cingulate activity as a predictor of degree of treatment response in major depression: evidence from brain electrical tomography analysis. JAMA Psychiatr 2001;158(3):405–15.

[46]. Mayberg HS, Brannan SK, Mahurin RK, Jerabek PA, Brickman JS, Tekell JL, et al. Cingulate function in depression: a potential predictor of treatment response. Neuroreport 1997;8(4):1057–61. [PubMed: 9141092]

[47]. Baxter LR, Schwartz JM, Phelps ME, Mazziotta JC, Guze BH, Selin CE, et al. Reduction of prefrontal cortex glucose metabolism common to three types of depression. Arch Gen Psychiatr 1989;46(3):243–50. [PubMed: 2784046]

[48]. Bench CJ, Friston KJ, Brown RG, Scott LC, Frackowiak RS, Dolan RJ. The anatomy of melancholia–focal abnormalities of cerebral blood flow in major depression. Psychol Med 1992;22(03):607–15. [PubMed: 1410086]

[49]. George MS, Wassermann EM, Williams WA, Callahan A, Ketter TA, Basser P, et al. Daily repetitive transcranial magnetic stimulation (rTMS) improves mood in depression. Neuroreport 1995;6(14):1853–6. [PubMed: 8547583]

[50]. George MS, Wassermann EM, Kimbrell TA, Little JT, Williams WE, Danielson AL, et al. Mood improvement following daily left prefrontal repetitive transcranial magnetic stimulation in patients with depression: a placebo-controlled crossover trial. JAMA Psychiatr 1997;154(12): 1752–6.

[51]. George MS, Nahas Z, Molloy M, Speer AM, Oliver NC, Li XB, et al. A controlled trial of daily left prefrontal cortex TMS for treating depression. Biol Psychiatr 2000;48(10):962–70.

[52]. George MS. Transcranial magnetic stimulation for the treatment of depression. Expert Rev Neurother 2010;10(11):1761–72. [PubMed: 20977332]

[53]. Conway CR, Chibnall JT, Gangwani S, Mintun MA, Price JL, Hershey T, et al. Pretreatment cerebral metabolic activity correlates with antidepressant efficacy of vagus nerve stimulation in treatment-resistant major depression: a potential marker for response? J Affect Disord 2012;139(3):283–90. [PubMed: 22397889]

[54]. McGrath CL, Kelley ME, Holtzheimer PE, Dunlop BW, Craighead WE, Franco AR, et al. Toward a neuroimaging treatment selection biomarker for major depressive disorder. JAMA Psychiatr 2013;70(8):821–9.

[55]. Keren NI, Lozar CT, Harris KC, Morgan PS, Eckert MA. In vivo mapping of the human locus coeruleus. Neuroimage 2009;47(4):1261–7. [PubMed: 19524044]

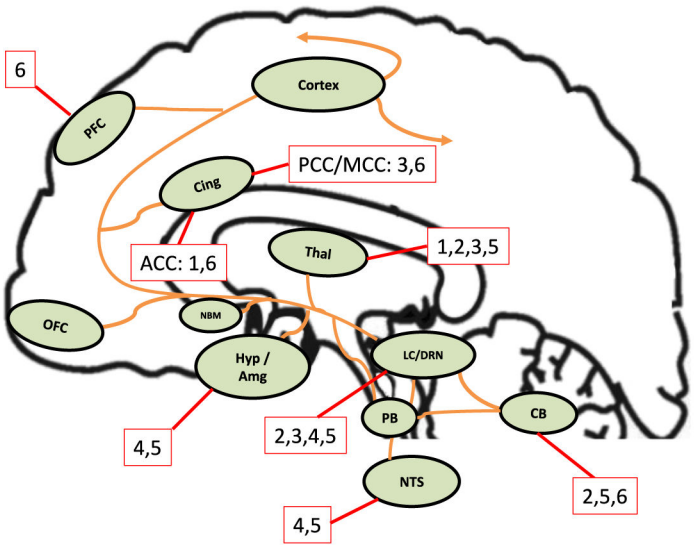

taVNS/fMRI studies

	First Author	Pulse Width	Frequency	On/Off time
1	Kraus, 2007	20μs	8Hz	30s On 120s Off
2	Dietrich, 2008	250s	25Hz	50s On 100s Off
3	Kraus, 2013	20μs	8Hz	30s On 60s Off
4	Frangos, 2015	250μs	25Hz	7min On 11min Off
5	Yakunina, 2016	500μs	25Hz	6min ON 90s Off
6	Badran, 2017 (this manuscript)	500μs	25Hz	60s On 60s Off

Numbers on figure represent increased BOLD signal activation in labeled brain regions and correspond to the table of taVNS/fMRI studies listed above

Fig. 1. Afferent pathway of the vagus nerve and regions activated by taVNS/fMRI studies.

Areas of the brain involved in the afferent vagal pathway. Nucleus tractus solitarius (NTS), locus coeruleus (LC), cerebellum (CB) thalamus (Thal), hypothalamus (Hyp), amygdala (Amg), and nucleus basalis (NBM) orbital frontal cortex (OFC), cingulate cortex (Cing), and prefrontal cortex (PFC). Effects are not limited to the named structures, as there are unlisted widespread, diffuse cortical effects (Cortex). Numbers labelling relevant regions of brain activations determined by corresponding study listed in adjacent table.

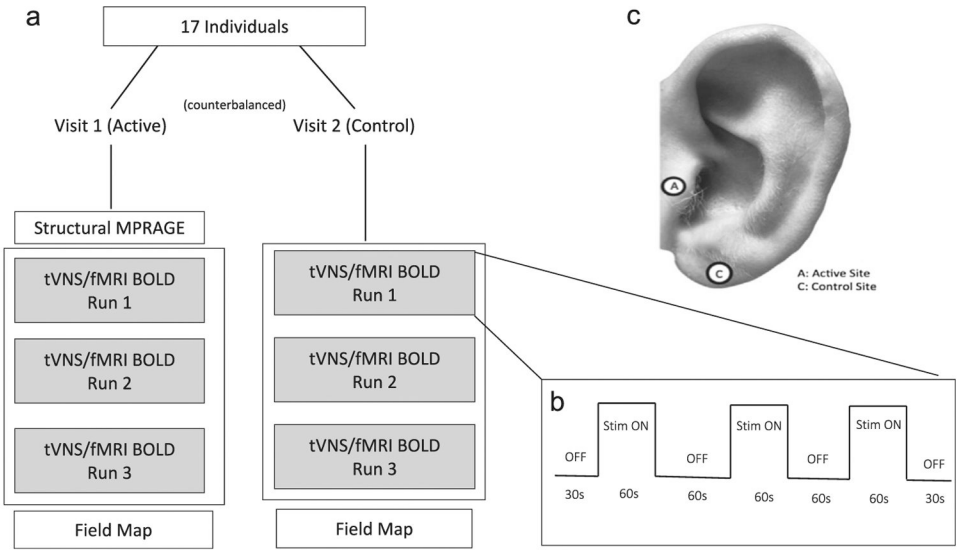

Fig. 2. Imaging study design.

a) Overview of scanning visits and MRI scans acquired. **b**) Block design of the concurrent taVNS/fMRI BOLD scans with stimulation times for “ON” and “OFF” blocks. **c**) Ear stimulation targets.

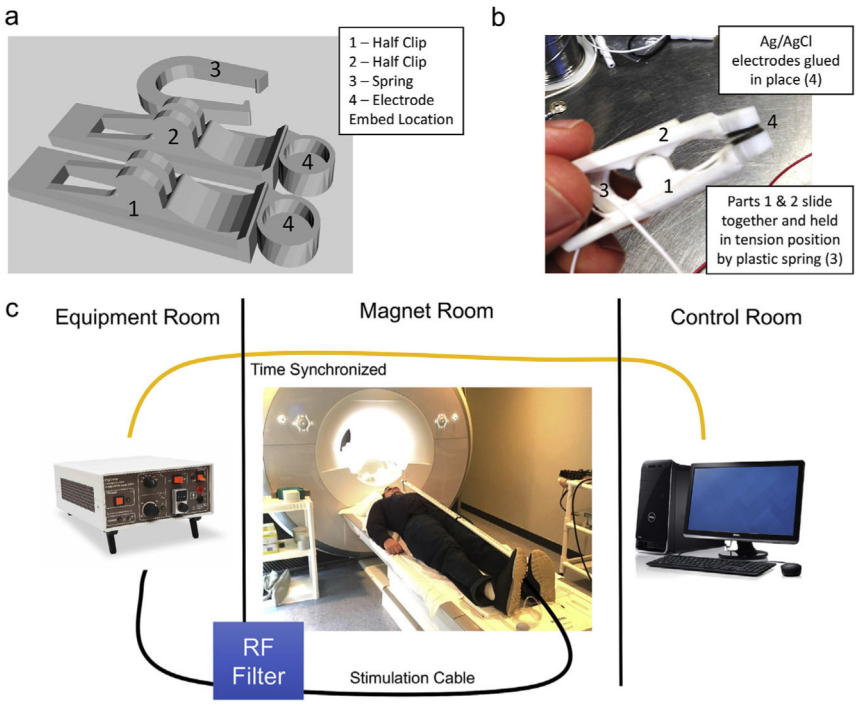

Fig. 3. taVNS/fMRI system overview.

a) picture of final taVNS electrodes that have been 3d printed and assembled **b**) CAD drawings of electrodes demonstrating the 3-piece design and “U” shaped spring clip. Ag/AgCl electrodes were affixed to the inside part of the electrode clips. **c**) Overview of how taVNS is synchronized and delivered to the participant in the fMRI scanner. Timing is driven from the console computer. Triggering of the direct current stimulator occurs in the equipment room which propagates an electrical stimulation current through a grounded RF filter and into the magnet room through a 10 m cable that attaches to the participant's ear in the scanner.

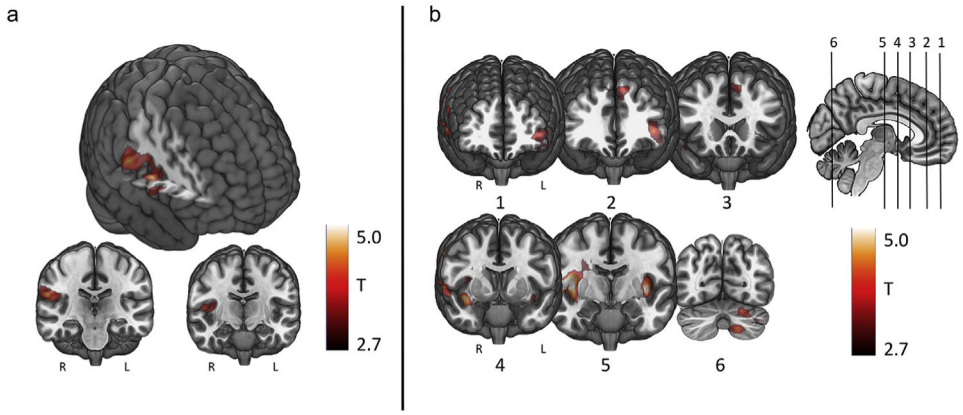

Fig. 4. Control and active stimulation findings.

a) Control stimulation only fMRI BOLD activations (compared to rest). (n = 17, one sample t-test, cluster FEW p < .05, cluster forming threshold p < .005, extent threshold = 100 voxels). **b**) Tragus stimulation only fMRI BOLD activations (compared to rest) (n = 17, one sample *t*-test, cluster FWE p < .05, cluster forming threshold p < .005, extent threshold = 100 voxels).

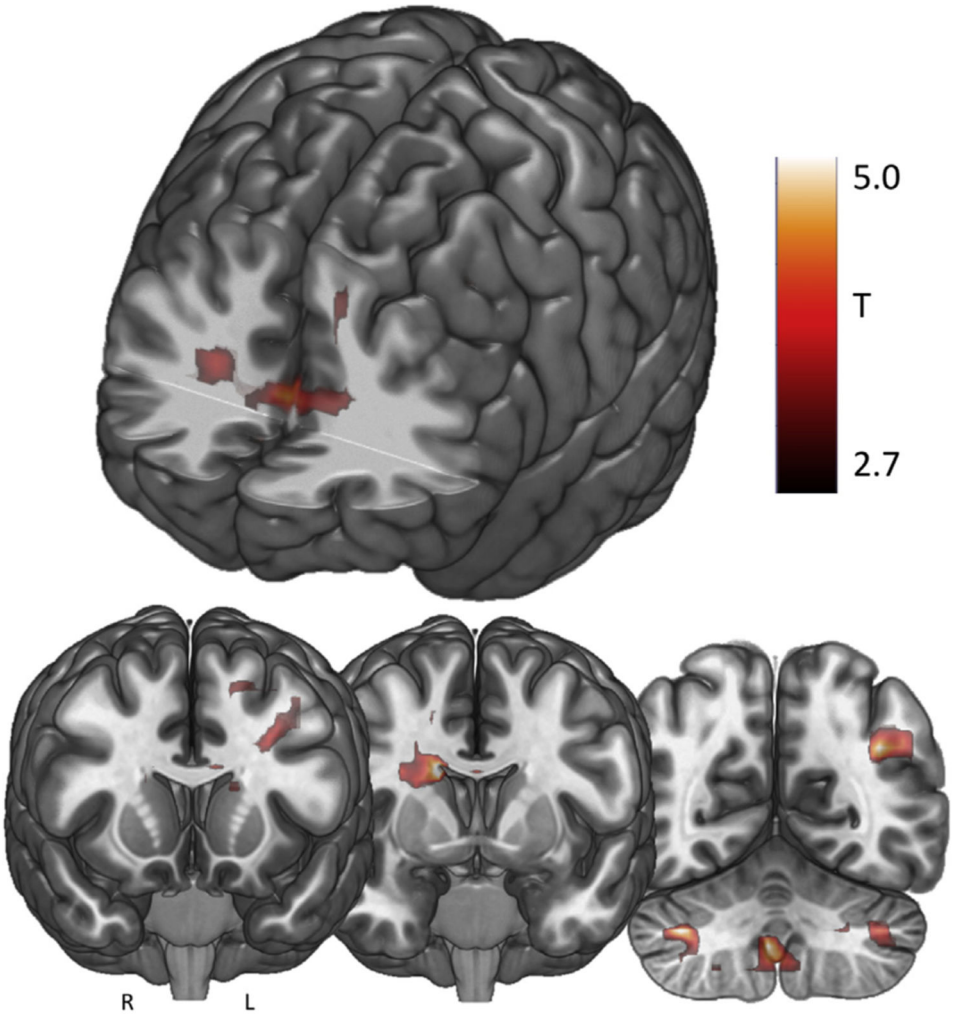

Fig. 5. Active stimulation > control stimulation findings.

fMRI BOLD activations resulting from the contrast active > control stimulation only. (n = 17, paired sample *t*-test, cluster FWE p < .05, cluster forming threshold p < .005, extent threshold = 100 voxels).

Table 1

Mean PT, current, and pain ratings during stimulation.

	Tragus (Active)	Earlobe (Control)	Significant? (p value)
PT ± SD (mA)	1.57 ± 0.48	1.22 ± 0.58	N
Stim. Current ± SD (mA)	3.14 ± 0.99	2.43 ± 1.16	
Mean 500 μs 25 Hz NRS Pain Rating ± SD	2.1 ± 0.87	1.43 ± 0.68	Y(p <.01)

Table 2

taVNS/fMRI Findings. Results from GLM analyses for active and control stimulation.

Cluster statistics			Cluster locations	Peak location (MNI)		
$P_{FWE-corr}$	# voxels	$p_{uncorrected}$		x	y	z
Left Earlobe (Control) Stimulation						
0.007	165	0.001	Right Central Operculum	48	−4	8
			Right Postcentral Gyrus	63	−16	23
			Right Insula	36	−13	17
Left Tragus(Active) Stimulation Only						
0	1491	0	Right Insula	36	−13	17
			Right Central Operculum	48	−7	8
			Right Postcentral Gyrus	60	−16	32
0.011	359	0.001		−36	−16	11
			Left Insula	−39	−7	2
				−39	2	−10
0.007	392	0	Left Angular Gyrus	−42	41	−1
			Left Inferior Frontal Gyrus	−48	44	−16
				−36	50	−16
0.077	221	0.005	Left Supplementary Motor Area	−9	23	47
			Left Superior Frontal Gyrus	−9	38	47
			Right Superior Frontal Gyrus	−9	35	47
0.082	217	0.006	Left Cerebellum	−15	−70	−46
Active Stimulation > Control Stimulation						
0.005	369	0		27	−7	35
			Right Caudate	15	2	23
			Right Mid Cingulate Gyrus	18	−4	38
0	698	0	Bilateral Cerebellum	3	−58	−43
			Right Cerebellum	36	−58	−37
			Left Cerebellum	−18	−67	−40
0.007	353	0	Bilateral Anterior Cingulate	3	35	11
			Left Anterior Cingulate	−12	26	17

Brain Stimul. Author manuscript; available in PMC 2019 April 29.

Cluster statistics			Cluster locations	Peak location (MNI)		
$P_{FWE\text{-}corr}$	# voxels	$p_{uncorrected}$		x	y	z
			Left Mid Cingulate	−9	14	23
0.053	221	0.003	Left Mid Frontal Gyrus	−30	14	35
			Left Superior Frontal Gyrus	−12	26	44
			Left Superior Frontal Gyrus	−12	38	35

Table 3

Prior taVNS/fMRI Trials.

taVNS/fMRI studies							
Year	**Author**	**n**	**Subjects**	**Site**	**Parameters**	**Control Condition**	**Findings**
2007	Kraus et al.	22	Healthy Controls	Outer ear Canal	20 μs 8 Hz 30s On 120s Off	Yes Earlobe	-Tragus > Control: BOLD ↓ in limbic (amg, hp, parahp g) and the MTG, STG BOLD ↑ in insula, PreCG, thal, R ACC **- Controlled pilot trial**
2008	Dietrich et al.	4	Healthy Controls	Inner Tragus	250 μs 25 Hz 50s On 100s Off	No	-Tragus > Control: BOLD ↑ in L LC, L > R thal, L PFC, Bl PcG, L PCG, L insula BOLD ↓ in R Nacc, R Cb **- Open-label pilot showing feasibility**
2013	Kraus etal.	16	Healthy Controls	Tragus vs Post ear canal	20 μs 8 Hz 30s On 60s Off	Yes Earlobe	-Tragus > Control: BOLD ↓ in parahp g, PCC, R thal (pulvinar), LC. -Tragus and Post ear canal > Control: BOLD ↑ in insula **- Tragus is optimal vagal stim site**
2015	Frangosetal.	12	Healthy Controls	L Conchae	250 μs 25 Hz 7 min On 11min Off	Yes Earlobe	BOLD ↑ signal in L NTS, Bl STN, DR, LC, R PBA, Amg, Nacc, bl paracentral lobule BOLD ↓ in hp, hypo **- L conchae is optimal vagal stim site**
2016	Yakunina et al.	37	Healthy Controls	4 ear targets	500 μs 25 Hz 6min On 90s Off	Yes Earlobe	Conchae Tragus > Control: BOLD ↑ NTS and LC, caudate, cb, hypo, thal, put **- Both conchae and tragus are active vagal sites**
2017	Badran et al. (this study)	17	Healthy Controls	Tragus	500 μs 25 Hz 60s On 60s Off	Yes Earlobe	Tragus > control = ↑ BOLD Caudate, Bl mid cing, R Caudate, Bl Cb, Bl ACC, L MFG, L SFG **- Tragus is optimal stim site for ACC, frontal, vagal activations**

Bl-bilateral; L-left; R-right; Stim- Stimulation.

Brain areas: MFG - Middle Frontal Gyrus; NTS-Nucleus of Solitary Tract; LC-Locus Coeruleus; thal – thalamus, PFC-prefrontal cortex, PreCG- Precentral gyrus; PostCG-Postcentral Gyrus; PCG-posterior cingulate gyrus; ACC – anterior cingulate cortex, Nacc- Nucleus Accumbens; PBA- Parabrachial area; Cb- Cerebellum, Hypo – hypothalamus, put – putamen, SF – superior frontal gyrus.